



*Dedicated to Professor Alexandru T. Balaban  
on the occasion of his 80<sup>th</sup> anniversary*

## SOAP FREE EMULSION POLYMERIZATION. A SPIN PROBE STUDY OF THE COLLOID SYSTEM IN THE EARLY STAGES OF REACTION

Adina ROGOZEA,<sup>a</sup> Florenta SAVONEA,<sup>a</sup> Agneta CARAGHEORGHEOPOL,<sup>a\*</sup>  
Ioneta-Codrina BUJANCA<sup>b</sup> and Mihai DIMONIE<sup>b</sup>

<sup>a</sup>“Ilie Murgulescu” Institute of Physical Chemistry, Roumanian Academy, Spl. Independentei 202, 060021 Bucharest, Roumania

<sup>b</sup>National Institute for Research and Development in Chemistry and Petrochemistry-ICECHIM Bucharest, Spl. Independentei 202, 060021 Bucharest, Roumania

*Received April 27, 2010*

Surfactant free emulsion polymerization (SFEP) is the only way to prepare “clean” organic polymer nanoparticles, free of surface-active agents, a property which may be important in certain applications, such as the synthesis of polymer composites. In the same time it is the simplest model for the study of emulsion polymerization mechanisms, which are still debated in the recent literature. In this paper we have used the capacity of the spin probe technique to identify and characterize colloidal species in order to evidence intermediate species during SFEP processes. Polymerization of styrene, methyl methacrylate and copolymerization of these monomers has been studied by introducing spin probes in aliquotes of the reaction mixture extracted at different moments, during reaction. The initiator used was potassium persulfate (KPS). Several reaction stages have been evidenced, such as the formation of surface-active oligomers, their concentration increase and assembling. Two important self-assembled species have been identified: (i) small, open aggregates of a few oligomers and (ii) oligomer-stabilized styrene mini droplets, in which the progress of polymerization could be followed. The proof of the existence of these intermediate species should contribute to the understanding of the SFEP mechanism.

### INTRODUCTION

Soap-free emulsion polymerization (SFEP), reported by Kotera *et al.*<sup>1</sup> in 1970 is the only way to prepare “clean” organic polymer nanoparticles, free of surface-active agents. The process is applicable only for monomers scarcely soluble in water (*e.g.* styrenes, alkyl methacrylates, etc.) and was mostly used for styrene. The particle size of the microspheres produced by SFEP is closely related to the nucleation mechanism. In this context, the role of ionizable initiators, such as potassium persulfate (K<sub>2</sub>S<sub>2</sub>O<sub>8</sub>) has been studied extensively.<sup>2-5</sup> Polymerization starts by addition of a sulfate radical to some of the monomers dissolved in water. The resulting charged oligomers behave as surfactants when reaching a certain length. The role played by

these surface-active oligomers in generating and stabilizing the emulsion is unanimously accepted. From here on there are different proposed mechanisms, some suggesting that polymerization takes place in micelles formed by the oligomers,<sup>2</sup> other ones considering styrene mini droplets as the reaction site.<sup>6,7</sup>

More recently the topic returned to attention, partly in connection with synthesis of polymer-silica composites.<sup>8-10</sup> Studies concerned with effects of co-monomers and additives, were also reported.<sup>8</sup> A large number of investigations of the polymerization have been carried out so far, mostly following the macroscopic characteristics of the system.<sup>11-15</sup> Recently Yamamoto *et al.*<sup>16,17</sup> have proposed a new model for SFEP, on basis of atomic force microscopy (AFM) data, involving

\* Corresponding author: acaraghe@icf.ro

small oligomer aggregates as the main polymerization site along with styrene mini-droplets.

The scope of this study is to describe the phase components of the reaction mixture at different stages of the SFEP process, with emphasize on the early stages, by electron paramagnetic resonance (EPR) of spin probes. The spin probe technique requires the introduction of stable nitroxide radicals into the studied system to obtain information about the local values of certain structural parameters (polarity, viscosity, order and dynamics). Depending on their hydrophile/hydrophobe or amphiphile character, spin probes are located in different microphases and report about the local nature, properties and about the ongoing processes. It has been proven that this methodology can significantly contribute to the detailed understanding of the local structural and dynamic parameters in micro-heterogeneous systems such as micellar solutions, microemulsions, lyotropic liquid crystals, vesicles, etc.<sup>18-20</sup> It was thus considered adequate for identifying and describing the aggregates present in the polymerization reaction mixture.

The envisaged results should or should not support the existence of certain intermediates proposed in the literature and shall contribute this way to the elucidation of the reaction mechanism.

## EXPERIMENTAL

**1. Materials.** The initiator:  $K_2S_2O_8$  (potassium persulfate) (KPS) (Aldrich) was used as received; the monomers styrene and methyl methacrylate (MMA) from Aldrich were purified by vacuum distillation. The spin probes used were 5-doxyl stearic acid (5DSA) from SIGMA-Aldrich and TEMPO – laurate (C12-NO) previously prepared as described in literature<sup>19</sup> (Fig. 1).

**2. Polymerization.** The emulsion polymerization of styrene, of MMA or their copolymerization in different proportions was performed in a reactor equipped with a stirrer and a nitrogen gas inlet, immersed in a thermostated water-bath. Styrene (or MMA) / water mixtures (2mL/25mL) were used, to which the initiator KPS ( $5.5 \times 10^{-3} M$  vs water) was added under stirring. An experiment with a 10 times higher initiator concentration ( $5.5 \times 10^{-2} M$  vs water) has also been conducted. The reaction mixture was deoxygenated by nitrogen bubbling for 30' under stirring and then heated to 70°C. The working temperature was reached in 15 minutes. All parameters of the polymerization reaction (stirring, heating, flask geometry, reagent quantities, etc.) have been strictly reproduced in all experiments. In the copolymerization reactions styrene was substituted with the same volume of a styrene/MMA mixture in 1:1 or 9:1 (v/v) proportion. Generally, the experiments have been repeated 3-4 times to assure reproducibility. For EPR measurements 1 mL aliquots were extracted from the reactor

at several time intervals and quickly cooled to RT. The polymerization recipes of the examined systems are given in Table 1.

**3. EPR measurements.** The EPR spectra were recorded in melting point capillary tubes at X-band, using a JEOL JES FA100 spectrometer. In our case the annihilation of the spin probe radicals during reaction had to be avoided. Therefore, the spin probes could not be introduced in the reaction mixture during reaction and were added after cooling the sample to room temperature (22-25°C).

Two spin probes have been used: TEMPO – laurate (C12-NO) and 5-doxyl stearic acid (5DSA) (Fig. 1). The spin probes were introduced from  $10^{-2} M$  stock solutions in ethanol so as to produce overall concentrations of  $2 \times 10^{-4} M$  (unless otherwise specified). EPR spectra of these samples were measured immediately and in some cases after several hours and on the next day.

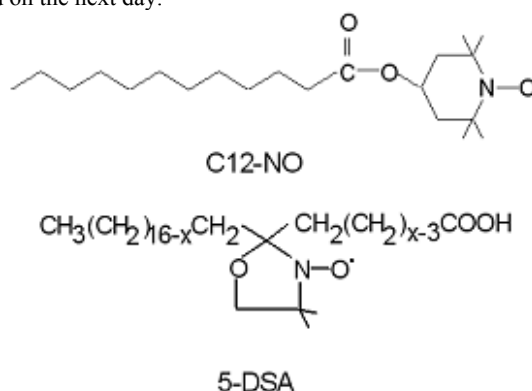


Fig. 1 – The spin probes used in this work: TEMPO-laurate (C12-NO) and 5-doxylstearic acid (5-DSA).

The information contained in the EPR spectra has been exploited in several ways. The  $^{14}N$  isotropic hyperfine splitting,  $a_N$ , which depends on the local polarity, was used to identify the composition of the components in the micro-heterogeneous system. The rotational correlation time,  $\tau_c$ , may be considered a relative measure of the local viscosity. Approximate  $\tau_c$  values were calculated according to the formula:<sup>21</sup>

$$\tau_c = (6.5 \times 10^{-10}) \Delta H(0) \{ [h(0)/h(-1)]^{1/2} + [h(0)/h(1)]^{1/2} \} \text{ sec}$$

where  $\Delta H(0)$  is the line width (in Gauss) of the central line and  $h(-1)$ ,  $h(0)$  and  $h(1)$  are the peak-to-peak heights of the  $M = -1$ ,  $0$  and  $+1$  derivative lines. This formula is correct for fast motion spectra that is, for  $\tau_c$  values which do not significantly exceed  $10^{-9}$  sec. The higher values in the Tables are only reported to signal important viscosity increases. The  $\tau_c$  value of spin probes in experimental spectra can thus be used to track viscosity changes in monomer droplets, following this way the progress of polymerization in time. When overlapped spectra were obtained, a deconvolution program<sup>22</sup> was used to separate them into components, for further analysis. Simulation of slow motion spectra using the program of Budil and Freed<sup>24,25</sup> yielded the exchange rate by bimolecular collisions ( $W_{ex}$ ), a value proportional to the local concentration of radicals.

## RESULTS

It is generally accepted that polymerization with KPS as initiator starts by the addition of a sulfate

radical to monomers dissolved in water in equilibrium with the bulk monomer phase. Charged oligomers result, which become surface-active at a certain chain length. The aqueous phase resembles at that moment a micellar solution of an ionic surfactant. Therefore, before describing the results obtained for each of the studied systems, it is instructive to follow the behavior of a model micellar system, earlier studied by Baglioni *et al.*<sup>23</sup>: a solution of sodium dodecyl sulfate (SDS) in

water, in which the evolution of C12-NO spectra is followed, as a function of SDS concentration: below critical micellar concentration (*cmc*), at *cmc* and above *cmc*. Here we have extended their study by using different spin probe concentrations, and analyzing the spectra by deconvolution and simulation. This approach was chosen in order to get support for the assignment of certain spectra observed in the preliminary phases of polymerization.

Table 1

Examined systems

Polymerization system	Monomer(s)/water 2mL/25mL	KPS <sup>a</sup> , mmol/L
A	Styrene	5.5
B	Styrene	55.0
C	MMA	5.5
D	styrene/MMA 9:1	5.5
E	styrene/MMA 1 : 1	5.5

<sup>a</sup> Initiator concentration is calculated relative to water

### 1. The SDS/water model system

The EPR spectra of C12-NO in several SDS solutions are illustrated in Fig. 2: for SDS concentration under critical micellar concentration (*cmc*) (Fig. 2a), at *cmc* (Fig. 2b), above *cmc* (Fig. 2c) and far above *cmc* (Fig. 2d). Several spin probe concentrations have been used (Table 2) in order to evidence the spin-spin exchange effects.

The spectral evolution can be understood taking into consideration that C12-NO is water-insoluble, amphiphilic and dissolves well in SDS micelles. Below the *cmc* of SDS the probe spectrum is a unique, not very broad line, which comes from C12-NO self-aggregation forming its own micelles. In these aggregates the radical moieties are very close to each other and spin-spin exchange phenomena appear, characterized by the exchange integral  $J=hW_{ex}$ , where  $W_{ex}$  is the exchange frequency due to bimolecular collisions. The effect of spin-spin exchange is to decrease the hyperfine splitting  $a_N$  and broaden the lines as the exchange frequency increases until the collapse of the three lines in a single one ("exchange narrowed") as in Fig. 2a. Obviously, the exchange frequency increases with the spin probe *local* concentration.

For SDS concentration equal to *cmc* a very specific broadening of spectral lines appears (Fig. 2b). For higher SDS concentrations exchange effects are gradually diminishing (Fig. 2c) and for SDS concentrations far over *cmc* the three sharp line spectrum observed is characteristic for the isolated spin probe, *i.e.* only one spin probe/micelle (Fig. 2d).

The peculiar spectrum at *cmc* proved to be a composite spectrum. Thus, spectral deconvolution<sup>22</sup> (Fig. 3a) has yielded two components: (1) a component with three narrow lines ( $a_N = 16.4$  G,  $\tau_C = 2.2 \times 10^{10}$ sec) whose characteristics correspond to the spectrum Fig. 2d, *i.e.* to isolated spin probes in SDS micelles, and (2) a spectrum of three very broad lines (Fig. 3b). The line broadening arises from spin – spin exchange<sup>23</sup> and could be simulated with the NLSL program<sup>24,25</sup> using large line widths and non-zero spin-spin exchange (Table 2).

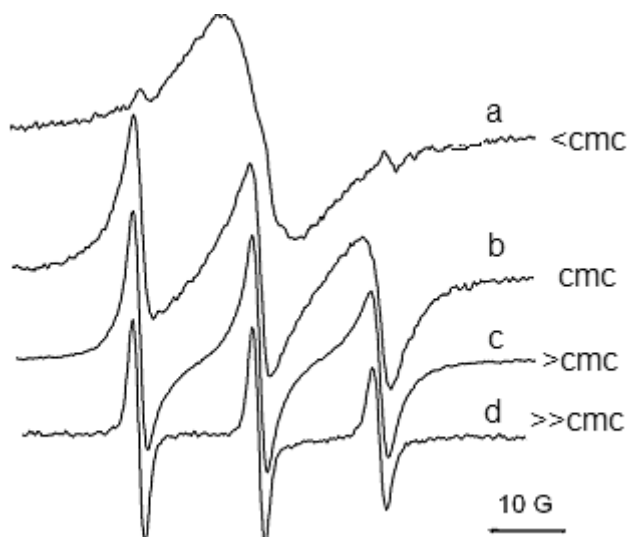


Fig. 2 – EPR spectra of C12-NO in aqueous solutions with increasing SDS concentration: (a)  $1 \times 10^{-3}$  M; (b)  $8.3 \times 10^{-3}$  M (*cmc*); (c)  $1 \times 10^{-2}$  M; (d)  $5 \times 10^{-2}$  M.

Table 2

Results of spectral deconvolution and spectra simulation for C12-NO in SDS/water solutions

[C12-NO] ( $10^{-3}$ M)	[SDS] ( $10^{-3}$ M)	%broad line	log $W_{ex}$
0.2	1	100	8.6
	8 <sup>a</sup>	68	7.0
	10	10	
	50	0	
0.5	1	100	8.7
	8 <sup>a</sup>	76	7.7
	10	63	
	50	0	
0.8	8 <sup>a</sup>	85	7.8
	10	82	

<sup>a</sup> *cmc* concentration of SDS

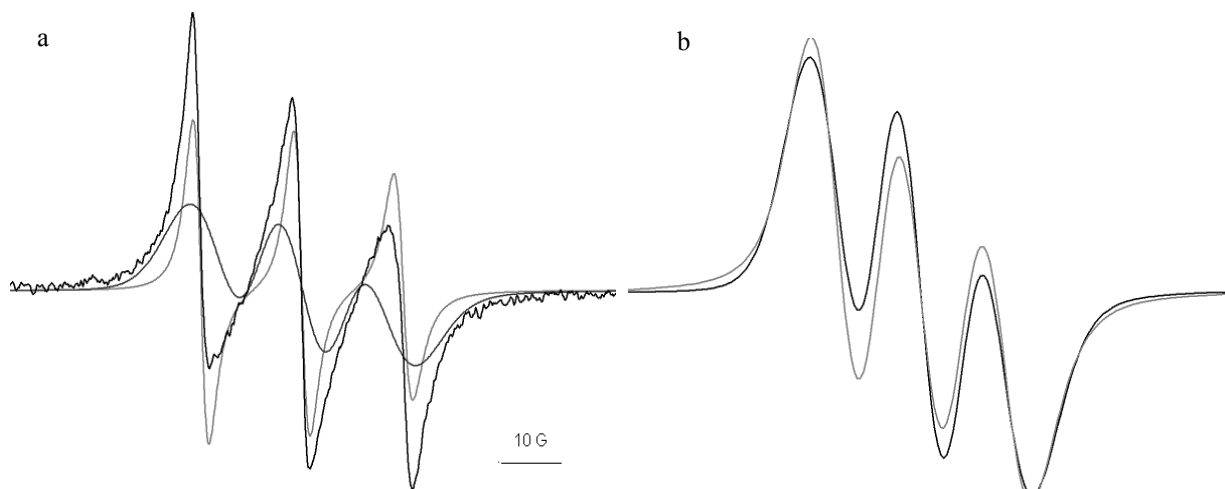


Fig. 3 – (a.) EPR spectrum of C12-NO ( $5 \times 10^{-4}$  M) in SDS  $8.3 \times 10^{-3}$  M (fat line) and its deconvolution into two components: (1) a spectrum of three narrow lines and (2) a spectrum of three broad lines; (b) simulation of spectrum (2) with resulting exchange rate  $\log W_{ex} = 7.7$ .

The broad line comes from aggregates in which more than one spin probe is dissolved, in fact mixed SDS-C12-NO micelles. Thus, it reflects the situation in which the concentration of surfactant micelles is smaller than the concentration of the spin probe. The ratio of the double integrals of the two spectra yields the proportion of each species in the mixture. The spectral parameters obtained from simulation indicate that, as expected, the percentage of the broad line as well as the spin-spin exchange frequency increase with the spin probe concentration, for a constant SDS concentration (Table 2). With increasing SDS concentration the proportion of the broad line diminishes gradually from 100% below *cmc* to 76% at *cmc* and to zero at high SDS concentration (Table 2) (Fig. 2c, 2d), due to the reduction of the spin probe local concentration as the number of SDS micelles increases. The observation of these effects opens the possibility to monitor – in the following – the concentration range of the surface active oligomers formed at different stages of the polymerization.

## 2. System A. Styrene / water / potassium persulfate (KPS) ( $5.5 \times 10^{-3} \text{M}$ )

EPR spectra of C12-NO ( $2 \times 10^{-4} \text{M}$ ) have been measured in samples extracted from the polymerization mixture at different time intervals (named after the time when extracted) (Fig. 4). The spectral parameters are reported in Table 3. Important changes have been observed over short time intervals. The spectra of samples extracted at 20' and 30' are similar with those in SDS at

concentrations below and respectively equal to *cmc* (Fig. 2a and 2b) and were assigned correspondingly. Thus, one can conclude that after 20' there are not yet enough surface-active oligomers to form micelles, but at 30' their concentration in the reaction mixture is close to their *cmc*.

Spectral deconvolution of the 30' spectrum (Fig. 5a) resulted in a narrow line triplet (similar to the 40' spectrum) and a broad line triplet. The last one has been simulated (Fig. 5b) and yielded an exchange rate  $\log W_{ex} = 8.3$ , far larger than for SDS at *cmc* (both obtained at the same overall spin probe concentration).

The 40' and 60' spectra (the last not shown in Fig. 4) consist of three equal, narrow lines – isolated spin probe – as expected for surface-active oligomer concentration far above *cmc*. However, the spectral parameters differ from those of spin probes in micelles in significant ways: the nitrogen *hfs*,  $a_N$ , value and the very small  $\tau_c$  value correspond to *bulk* styrene, whereas in micelles the  $\tau_c$  values would be significantly increased *vs* bulk. On the other hand micelles of ionic surfactants are known to dissolve only minute amounts of hydrocarbons in the core, which do not have the properties of bulk solvent. Thus, the aggregates observed over a significant reaction time interval (30'- 60') match rather the properties of oligomer stabilized styrene mini-droplets than micelles, and have been assigned as such (it is thus incorrect to refer to the concentration where both type of specimens coexist, as *cmc*. In the following this will be designated as “*cmc*”).

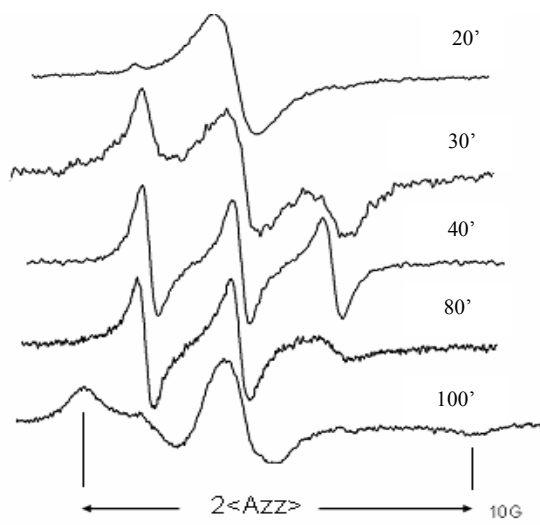


Fig. 4 – Polymerization A. C12-NO spectra at the indicated reaction times.

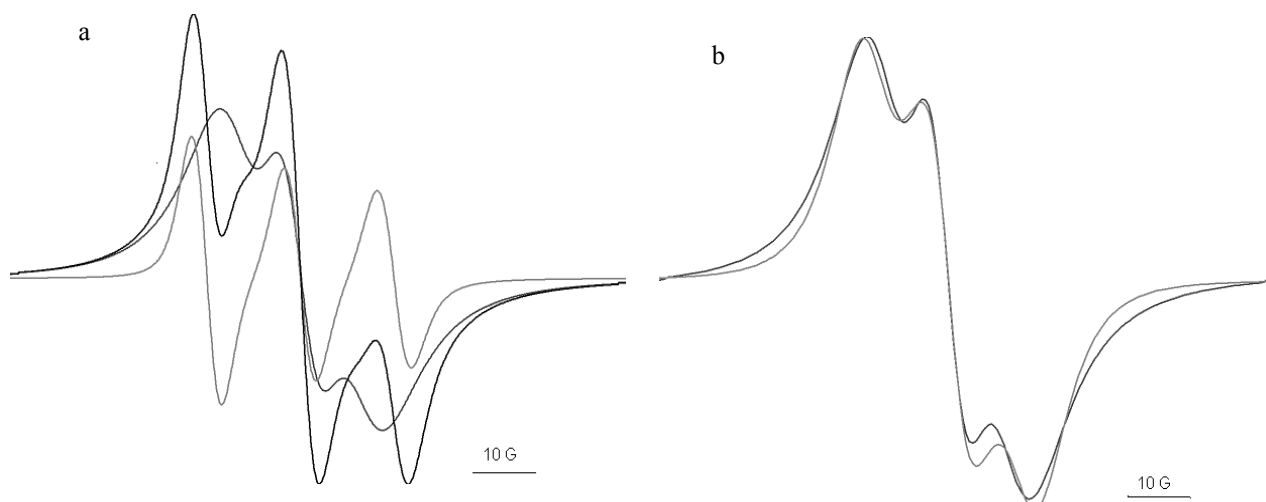


Fig. 5 – Polymerization A. (a) C12-NO in the 30' sample (fat line) and the spectra of components obtained after deconvolution (thin lines); (b) NLSL simulation of the broad line. The spin-spin exchange frequency found was  $\log W_{ex}=8.3$ .

This result shows that in the first 40' the number of surface-active oligomers increases and ensures the stabilization of styrene droplets.

After 80', the spectrum (Fig. 4) shows line broadening characteristic of a slower reorientation rate of the probe, due to local viscosity increase. The gradual viscosity increase in time suggests that the changes observed occur within the same colloidal specimen and most probably reflects the progress of styrene polymerization.

At 100' reaction time the spin probe is practically immobilized, the spectrum being characteristic for the spin probe in a solid.

The spectra of these samples did not change in time after being extracted from the reaction mixture.

### 3. System B. Styrene / water / potassium persulfate (KPS) ( $5.5 \times 10^{-2} \text{M}$ )

In system B a ten times higher initiator concentration has been used in order to observe the influence of a larger amount of surface-active oligomers on the reaction progress and to check the correctness of the previous assignments. The experimental procedure was the same as with system A. A first observation is that here, at variance with A, the reaction continues slowly for several hours after cooling to room temperature. Therefore, the evolution of the spectra has been followed until next day. Secondly, the time evolution of the reaction in system B is different from A (Fig. 6): at 20', the unique line spectrum of C12-NO self-aggregates does not appear, instead two overlapped three narrow-line spectra were observed.

The values found are 17.0 G and 15.4 G corresponding to water and to styrene, respectively.

Each spectrum has three equal lines indicating very low viscosity ("fast motion" regime). Left at room temperature for 24 h the sample has the same two spectra, but the styrene spectrum had a higher  $\tau_C$  ( $8.3 \times 10^{-10}$  sec) and a higher proportion in the mixture: 96%. For the 40' sample the contribution of the styrene spectrum is increased. Next day only the styrene type spectrum remained, and with a considerably reduced mobility (increased local viscosity) ( $\tau_C = 12.55 \times 10^{-10}$  sec) (Fig. 6). In the sample extracted at 80' the styrene line developed into a solid-type spectrum, but the water type spectrum was still present and corresponded to rapid movement. It disappeared until next day.

Since C12-NO is water insoluble, the narrow line spectrum with  $a_N = 17$  G (typical value for water) and  $\tau_C = 0.5 \times 10^{-10}$  sec (very high mobility) is assigned to small surface-active oligomer "nuclei" which help dissolve C12-NO, but let it exposed to water. When C12-NO is dissolved in a typical micelle, such as SDS, it does not have contact with water and its mobility is reduced (see the spectral parameters in the previous paragraph). These pre-micellar aggregates have been identified in the polymerization reaction at high KPS concentration during reaction time, and disappear gradually when generation of new radicals stops. Aggregates with a small number (13) of oligomers (MW=1000) have been previously mentioned in the literature.<sup>2,16</sup> Interestingly, in our case no changes in the spectral parameters of this specimen were observed during the reaction, or after. Thus, the "nuclei" do not change into real micelles, in spite of the continuous generation of oligomers. The last ones seem to be mostly involved in the stabilization of styrene droplets, where they are part of the polymerization process.

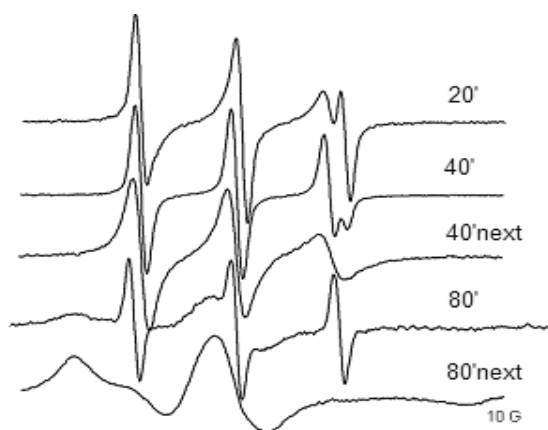


Fig. 6 – Polymerization B. Evolution of C12-NO spectra during the course of reaction.

The styrene type spectrum corresponds – as discussed for system A – to large aggregates containing styrene, that is, to styrene mini-droplets. At early reaction times the viscosity of these droplets is as low as in bulk styrene, but it increases in time, as reflected in the increasing  $\tau_C$  value. The change in C12-NO dynamics due to

local viscosity increase offers information on the evolution of polymerization in the styrene mini-droplets, which prevail in both A and B systems. In system B solid formation is observed already after 60', vs 100' in A, as a result of higher initiator concentration.

The experimental results are collected in Table 3.

Table 3

EPR data for C12-NO in styrene polymerization at different reaction times (A and B systems)

Sample extracted/measured	Spectrum Type/ (%)	$a_N$ (G)	$\log(w_{ex})$	$\tau_C$ ( $10^{-10}$ s)
<b>A Low concentration of KPS (<math>5.5 \times 10^{-3}</math>M)</b>				
20'	U		8.8	
20'/next day	U			
30'	U* / 58%		8.3	
	ST*			1.5
40'	ST	15.6		1.0.
40'/next day	ST	15.6		1.2
50'	ST			1.0
60'	ST	15.6		1.2
60'/next day	ST	15.6		1.2
80'	ST	15.6		22.5
100'	SLD			
		$2 \langle A_{zz} \rangle = 66.2$ G		
<b>B High concentration of KPS (<math>5.5 \times 10^{-2}</math>M)</b>				
20'	ST*	15.6		1.9
	W*/ 20%	17.1		0.5
20'/next day	ST*	15.6		8.6
	W*/ 4%	17.1		0.5
40'	ST*	15.6		2.0
	W*/ 9%	17.1		0.5
40'/next day	ST	15.6		12.9
60'	SLD	$2 \langle A_{zz} \rangle = 64.7$ G		
	W			
60'/next day	SLD	$2 \langle A_{zz} \rangle = 65.6$ G		
100'	SLD	$2 \langle A_{zz} \rangle = 66.0$ G		
	W			

\*overlapped spectra separated by deconvolution;

U – unique line, assigned to self-assembled micelles of the amphiphilic spin probe itself;

W – three sharp lines, with an  $a_N$  value corresponding to water polarity;

ST – a three line spectrum with  $a_N$  value corresponding to styrene polarity;

SLD – a solid type spectrum corresponding to an immobilized spin probe.

A second spin probe was used, 5-doxyl stearic acid (5-DSA), known to insert at interfaces in colloidal species. Fig. 7 illustrates the time evolution of 5-DSA spectra during polymerization in systems A: after 20' of reaction 5-DSA presents a fast motion spectrum in an aqueous environment. The EPR signal is intense, in spite of 5-DSA being very scarcely soluble in water, so this spectrum was assigned – as with C12-NO – to the spin probe included in small nuclei with few oligomers, where the spin probe remains in contact with water.

In all other samples from polymerization A and B, 5-DSA is localized in styrene environment (Table 4). The polar head of 5-DSA is usually located in the polar/nonpolar ordered interface of micelles or emulsion droplets, producing specific

spectra, reflecting the anisotropy of motion.<sup>26</sup> Such spectra have however not been observed in the styrene droplets formed. It appears that in these styrene droplets the oligomers – being of the same composition with styrene – do not form a separate ordered phase at the interface.

The  $\tau_c$  values – correlated with the local viscosity – increase in time due to polymerization progress. Similarly to C12-NO, 5-DSA becomes eventually immobilized (in system A after 80' and in system B after 60' of reaction). As expected, the two probes report similar data concerning the evolution of the viscosity in styrene mini-droplets.

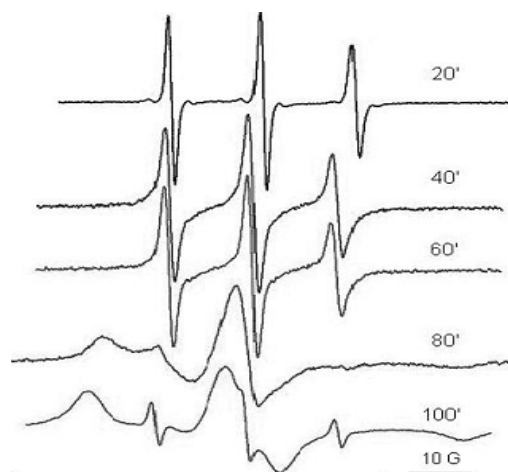


Fig. 7 – Polymerization A. 5-DSA spectra at the indicated reaction times.

Table 4

EPR data for 5-DSA during styrene polymerization, at different reaction times

(A and B systems)*				
Sample extracted/measured	Spectrum type	$a_N$ (G)	$2\langle A_{zz} \rangle$ (G)	$\tau_c$ ( $10^{-10}$ s)
<b>A Low KPS concentration (<math>5.5 \times 10^{-3}</math> M)</b>				
20'	W	15.8		1.7
20'/next day	W	15.8		1.7
40'	ST	14.5		4.0
40'/next day	ST	14.5		4.6
60'	ST	14.5		4.6
60'/next day	ST	14.5		5.3
80'	SLD		64.2	
<b>B High KPS concentration (<math>5.5 \times 10^{-2}</math> M)</b>				
20'	ST	14.5		3.8
40'	ST	14.4		4.7
40'/after 3h	ST	14.4		7.7
40'/next day	ST	14.4		14.3
60'	SLD		64.7	
60'/next day	SLD		64.7	
80'	SLD		64.7	

\*same abbreviations as in Table 3

#### 4. System C. Methyl methacrylate (MMA)/water/potassium persulfate (KPS) ( $5.5 \times 10^{-3} M$ )

MMA has a higher water solubility compared to styrene and this fact should influence the concentration of oligomers in the aqueous phase. Thus the study of MMA polymerization might provide a confirmation of the assignments made so far. Polymerization of MMA has been studied in a similar way with that of styrene. The results obtained with C12-NO spin probe are summarized in Table 5.

The following differences can be identified, compared to the analogous system A (same initiator concentration and quantity of monomer): (i) for MMA the single line at 20' does not appear,

that is, there are enough surface-active oligomers to dissolve C12-NO. This is what one expects considering the higher water-solubility of MMA; (ii) instead, after 20' of reaction a spectrum similar to that at 30' in Fig. 4 is observed indicating that the MMA oligomer concentration is around "cmc", which means that stabilized MMA mini-droplets are already being formed; (iii) after 40' the spin probe is already immobilized in the polymer matrix. The reaction is so rapid that the specific spectrum of the probe in liquid monomer droplets has not been observed. In conclusion, the polymerization of methyl methacrylate at low concentration of initiator goes through similar stages, but is much faster compared to styrene. Previous literature data have also reported this trend<sup>9</sup>.

Table 5

EPR data for C12-NO during MMA polymerization (system C) and styrene/MMA copolymerizations (systems D and E)\*

Sample	Spectrum type	$a_N$ (G)	$2\langle A_{zz} \rangle$ (G)	$\tau_C$ ( $10^{-10}s$ )
<b>C: MMA</b>				
20'	U <sup>a</sup> ST <sup>a</sup>	15.2		3.4
40'	SLD		66.2	
60'	SLD		66.0	
<b>D: styrene:MMA= 1:1</b>				
20'	U <sup>a</sup> ST <sup>a</sup>	15.4		3.3
40'	SLD		66.1	
60'	SLD		66.1	
<b>E: styrene:MMA=9:1</b>				
20'	U <sup>a</sup> ST <sup>a</sup>			
40'	ST	15.5		3.1
60'	SLD		63.6	
100'	SLD		63.8	

\*same abbreviations as in Table 3;

<sup>a</sup> after deconvolution

#### 5. Styrene/methyl methacrylate (MMA) copolymerizations

System D. Styrene: MMA = 1:1 (v/v)  
/water/potassium persulfate (KPS) ( $5.5 \times 10^{-3} M$ )

System E. Styrene: MMA= 9:1 (v/v)  
/water/potassium persulfate (KPS) ( $5.5 \times 10^{-3} M$ )

Two compositions with different monomer ratios have been selected for styrene/methyl methacrylate copolymerization. All results are collected in Table 5. Examination of the C12-NO spectra (not shown) in these two systems shows that system D behaves similarly with the one containing only MMA monomer (C system), with

the same sequence of spectra. On the other hand, system E with 90% styrene, is similar to A except that polymerization is more advanced at 60' due to the presence of MMA (the spin probe is in a solid-like environment), whereas for A this happens only after 80'.

#### DISCUSSION

Polymerization starts by addition of a sulfate radical to some of the monomers dissolved in water. The resulting charged oligomers behave as surfactants after reaching a certain length.

Two models are being discussed in the literature, regarding the mechanism of SPEF: (i). The micellar mechanism is based on the supposition that the oligomers formed in aqueous phase in the early stages of the polymerization are forming micelles.<sup>2,13</sup> Further, the reaction continues in micelles as in a conventional process: emulsion polymerization through micelle nucleation. (ii). The monomer mini-droplets mechanism considers that monomer mini-droplets are generated under stirring at the monomer/water interface and are stabilized by the adsorption of surface-active free-radical oligomers generated by the reactions in both aqueous phase and at the interface.<sup>6</sup> The monomer transfer from the bulk phase to the growing particles takes place via the coalescence of mini-droplets with particles. The sole role of the reaction in the aqueous phase would be to provide the surface-active oligomers for the stabilization of particles.<sup>7</sup>

Ou *et al.*<sup>11</sup> have indeed evidenced by gel permeation chromatography (GPC), in the early stage of polymerization the presence of oligomers having the molecular weight of about 1000.

More recently, Yamamoto *et al.*<sup>16,17</sup> have reached the following conclusions on basis of AFM data: there are two simultaneous mechanisms producing polystyrene particles in the polymerization: (1) the polymerization within monomer droplets fragmented by mixing from the main monomer phase, and (2) the polymerization of monomers dissolved in the aqueous phase by initiators. The “embryos” in this polymerization are estimated to be micelle-like aggregates of several oligomers composed of ca. 10 styrene repeating units with an initiator radical head. Mechanism (i) is normally neglected or not recognized because of the small contribution. The later process is regarded as the main production process of polystyrene particles.

Our results have shown that with styrene as monomer, at low KPS concentration the reaction is slow enough to allow the observation of several well separated reaction stages: (a) an induction phase, when the concentration of surface-active oligomers is too low for aggregates to be generated; (b) a starting phase, when small oligomer aggregates – so called “nuclei”<sup>13</sup> – with a fixed, open structure appear; no changes were observed in the structure of this species during reaction; (c) the concentration increase of the oligomers, until a stage is reached when oligomer-stabilized styrene mini-droplets appear; (d) a reaction phase when the styrene mini-droplets with

a liquid core prevail; (e) a final stage when the progress of polymerization in the mini-droplets is observed, as reflected in the gradual immobilization of the spin probes. With high initiator concentration the reaction rate increases and more than one of the processes described may take place simultaneously.

The methyl methacrylate monomer polymerizes faster than styrene (all reaction conditions being the same); the pre-micellar stage is not observed due to rapid formation of oligomers in high aqueous concentration; the monomer droplets polymerization occurs very fast, so that liquid core droplets are not observed.

In the copolymerization of styrene – MMA, 1:1 (v/v), the system behaves similarly to MMA, while, in the case of the 9:1 ratio the evolution of the reaction is similar to that of styrene.

It is remarkable that, while the timing and rate of development of the described phenomena present some variation as a function of initiator concentration, or the nature of the monomer(s), the structure and properties of the colloidal species involved in the reaction are the same in all investigated cases and have the same evolution.

While our data – based on EPR of spin probes – can only reflect certain aspects of the polymerization reaction, they have nevertheless clearly shown the basic components of the colloidal system and their time evolution.

On basis of these data, polymerization does not seem to take place by micellar mechanism since such aggregates have not been found; it seems to take place in the monomer mini-droplets stabilized by oligomers, as suggested in mechanism (ii).

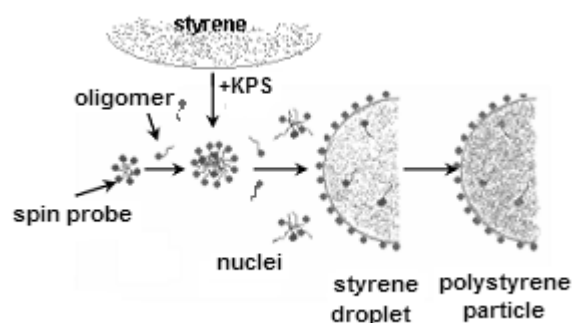


Fig. 8 – Schematic illustration of the colloidal species participating in the SFEP.

## CONCLUSIONS

EPR of spin probes was used to describe the components of the colloid system resulting during

SFEP of styrene, MMA and of their mixtures. The formation of oligomers with an ionic head, which behave as surfactants, as well as their concentration increase could be followed by specific spectra of two spin probes. The oligomers formed are leading to two colloid species which have been positively identified: (i) a pre-micellar, small, open aggregate of oligomers and (ii) oligomer-stabilized monomer mini-droplets, both of which have been reported in literature as intermediates to which different roles have been assigned (Fig. 8). The progress of polymerization in the mini-droplets could be observed by gradual spectral changes of the probe mobility in the droplet from a free-rotating to an immobilized entity. This behavior was specific for all investigated systems, regardless of the initiator concentration and with both styrene, MMA or in their copolymerization reaction. The experimental observations above suggest that polymerization mainly takes place in monomer mini-droplets.

*Acknowledgments:* This work was supported by CNCISIS (Roumania) grant 1132/2007.

## REFERENCES

1. A. Kotera, K. Furusawa and Y. Takeda, *Colloid Polym. Sci.*, **1970**, *239*, 677-681.
2. A. R. Goodall, M. C. Wilkinson and J. Hearn, *J. Polym. Sci. Polym. Chem.*, **1977**, *15*, 2193-2218.
3. M. Arai, K. Arai and S. Saito, *J. Polym. Sci. Polym. Chem.*, **1979**, *17*, 3655-3665.
4. M. Arai, K. Arai and S. Saito, *J. Polym. Sci. Polym. Chem.*, **1980**, *18*, 2811-2821.
5. D. Munro, A. R. Goodall, M. C. Wilkinson, K. Randle and J. Hearn, *J. Colloid Interface Sci.*, **1979**, *68*, 1-13.
6. S. Kozempel, "Emulsifier-free emulsion polymerization: monomer solution state and particle formation", PhD thesis, **2005**, University of Potsdam, Germany.
7. N. Hen-Mei, D. Yong-Zhong, M. Guang-Hui, N. Masatoshi and O. Shinzo, *Macromolecules*, **2001**, *34*, 6577-6585.
8. J. Lee, C. K. Hong, S. Choe and S. E. Shima, *J. Colloid. Interface Sci.*, **2007**, *310*, 112-120.
9. X. Pang, G. Cheng and S. Lu, *J. Appl. Polymer Sci.*, **2004**, *92*, 2675-2680.
10. M. Egen and R. Zentel, *Macromol. Chem. Phys.*, **2004**, *205*, 1479-1488.
11. J. L. Ou, J. K. Yang and H. Chen, *Eur. Polym. J.*, **2001**, *37*, 789-799.
12. H. S. Chang and S.A. Chen, *J. Polym. Sci. A: Polym. Chem.*, **1988**, *26*, 1207-1229.
13. Z. Song and G. W. Poehlein, *J. Colloid. Interf. Sci.*, **1989**, *128*, 501-510.
14. S. A. Chen and H. S. Chang, *J. Polym. Sci. A: Polym. Chem.*, **1990**, *28*, 1547-1561.
15. S. A. Chen and S. T. Lee, *Macromolecules*, **1991**, *24*, 3340-3351.
16. T. Yamamoto, Y. Kanda and K. Higashitani, *Langmuir*, **2004**, *20*, 4400-4405.
17. T. Yamamoto, M. Nakayama, Y. Kanda and K. Higashitani, *J. Colloid. Interface Sci.*, **2006**, *297*, 112-121.
18. A. Caragheorgheopol and H. Căldăraru, "Electron Paramagnetic Resonance", vol. 17, Royal Society of Chemistry, Cambridge, 2000, p. 205-245.
19. A. Caragheorgheopol, H. Căldăraru, I. Draguțan, H. Joella and W. Brown, *Langmuir*, **1997**, *13*, 6912-6921.
20. A. Caragheorgheopol, J. Pilar and S. Schlick, *Macromolecules*, **1997**, *30*, 2923-33.
21. T. J. Stone, T. Buckman, P. L. Nordio and H. M. McConnell, *Proc Natl Acad Sci U S A.*, **1965**, *54*, 1010-1017.
22. T.I. Smirnova and A.I. Smirnov, in "Biological Magnetic Resonance", vol.27, L. Berliner, New York, 2007, p. 165-251.
23. P. Baglioni, E. Ferroni, G. Martini and M.F. Ottaviani, *J. Phys. Chem.*, **1984**, *88*, 5107-5113.
24. D.E. Budil, S. Lee, S. Saxena and J.H. Freed, *J. Magn. Reson. A*, **1996**, *120*, 155-189.
25. D.J. Schneider and J.H. Freed, "Biological Magnetic Resonance", vol. 8, L. J. Berliner, New York, 1989, p. 1-76.
26. J.J. Seelig, "Spin Labeling", L.J. Berliner, New York, San Francisco, London, 1976, p. 373-409.

